# Single amino acid changes decouple two opposite activities of a viral auxiliary replication protein

Qin Guo[1], Shaoyan Zhang[1], Rong Sun[1], Xiaolong Yao[1], Satyanarayana Tatineni[2], Tea Meulia[1,3], and Feng Qu[1]*

[1]Department of Plant Pathology, [3]Molecular and Cellular Imaging Center, Ohio Agricultural Research and Development Center, The Ohio State University. Wooster, OH 44691.

[2]USDA-ARS and Department of Plant Pathology, University of Nebraska-Lincoln, Lincoln, NE 68583

*Primary contact: Feng Qu, qu.28@osu.edu; 330-263-3835

**ABSTRACT**

We recently reported that the auxiliary replication protein encoded by the single-stranded, positive sense RNA genome of turnip crinkle virus (TCV), designated p28, also repressed TCV replication under certain conditions, and this repressive function accounted for superinfection exclusion (SIE) among TCV variants. However, it was unknown whether the replication role of p28 could be molecularly separated from its opposite role of repressing replication. Here we report the identification of two single amino acid (aa) mutations that decouple these two functions. Using an *Agrobacterium* infiltration-based delivery system, we transiently expressed a series of p28 deletion and point mutants, and tested their ability to elicit SIE against a co-introduced TCV replicon. We found that substituting alanine (A) for valine (V) and phenylalanine (F) at p28 positions 181 and 182, respectively, modestly compromised SIE in transiently expressed p28 derivatives. Upon incorporation into TCV replicons, the V181A and F182A mutations decoupled TCV replication and SIE diametrically. While V181A impaired SIE without detectably compromising replication, F182A abolished TCV replication but had no effect on SIE once the replication of the F182A replicon was restored through complementation. Furthermore, F182A also decoupled the replicational roles of p28 and p88, the other TCV-encoded replication protein that encompasses p28, as the F182A replicational defect was readily complemented by transiently expressed p28, but not p88. Together our findings demonstrated that the replication and SIE functions of p28 were molecularly separable, and provided valuable resources for in-depth mechanistic dissections of SIE.

31 **IMPORTANCE**

32 Superinfection exclusion (SIE) insulates virus-infected cells from subsequent invasion by the same
33 or closely related viruses. SIE has been observed in both animal and plant virus-infected cells. Therefore,
34 a thorough understanding of how SIE is achieved at the molecular level is expected to inspire novel
35 strategies for combating virus infections in humans, animals, and plants. Our group has been using
36 turnip crinkle virus (TCV) to elucidate the molecular interactions critical for SIE elicitation. The current
37 study builds on our previous observation that TCV SIE is elicited by one single TCV-encoded protein
38 (p28), and further identifies key regions and amino acids that are needed for SIE. This study identifies
39 key amino acid changes that decouple the replication and SIE functions of p28, hence provides valuable
40 resources for in-depth mechanistic dissection of SIE.

41 **INTRODUCTION**

42 Many viruses block the subsequent entry and/or replication of the same or closely related viruses
43 in the cells they occupy, through a process known as superinfection exclusion (SIE). These viruses
44 include important human and animal pathogens such as human immunodeficiency virus (HIV), hepatitis
45 C virus (HCV), West Nile virus (WNV), and vesicular stomatitis virus (VSV) (1–5), as well as plant
46 pathogens like tobacco mosaic virus (TMV), citrus tristeza virus (CTV), cucumber mosaic virus (CMV),
47 wheat streak mosaic virus (WSMV), and turnip crinkle virus (TCV) (6–11). SIE in plant virus infections is
48 also thought to underlie the well-documented cross protection phenomenon (12–14). Cross protection
49 insulates plants from a disease-causing virus by simply pre-inoculating them with a mild variant of the
50 same virus. Although cross protection has been adopted for plant virus disease management for at least
51 50 years (12), its underlying molecular mechanism remains poorly understood.

52 A number of earlier studies investigated SIE of plant viruses by tagging the same virus with two
53 different fluorescent proteins (e.g. green fluorescent protein [GFP] and mCherry) (6, 7, 9, 10, 15, 16).
54 These studies demonstrated that most of the viruses excluded their own variants at the single cell level,
55 thus implicating intracellular exclusion as one of the primary causes for SIE. Using this approach, Zhang
56 and colleagues (15) found that SIE in TCV infections occurred inside individual cells, and it acted to block
57 the replication of the superinfecting TCV replicons. Strikingly, this replicational blockage was mediated
58 by p28, one of the TCV-encoded proteins required for TCV genome replication (15). The fact that p28,
59 the auxiliary replication protein of TCV, functions to both facilitate and repress the replication of TCV
60 genomic RNA (gRNA), along with the observation that fluorescent protein-tagged p28 formed large
61 intracellular bodies that coalesced other p28 variants, prompted the hypothesis that p28 undergoes
62 concentration-dependent conformational changes to accommodate its dual functions. Namely, the p28
63 protein assumes one conformation at lower concentrations to enable replication, but another self-
64 perpetuating conformation at higher concentrations to block replication (15, 17).

65 TCV is a small icosahedral plant virus with a (+)-strand RNA genome that encodes five proteins.
66 The 5' proximal p28 and its C-terminally extended derivative – p88 – are both translated directly from
67 TCV genomic RNA (gRNA), and are themselves required for gRNA replication (Fig. 1A). Since the
68 production of p88 depends on infrequent translational read-through of the p28 stop codon (UAG), the
69 intracellular concentration of p28 far exceeds that of p88 (18). However, p28 lacks the conserved RNA-
70 dependent RNA polymerase (RdRP) motif, is hence known as the auxiliary replication protein. On the
71 other hand, p88 is thought to be directly responsible for gRNA replication through its RdRP activity. TCV
72 additionally encodes two small movement proteins, p8 and p9, that are translated from subgenomic
73 RNA 1 (sgRNA1), and a capsid protein/silencing suppressor from sgRNA2 (Fig. 1A) (19–21).
74 In the recent study by Zhang and colleagues (15), we established that p28 was necessary and
75 sufficient to elicit SIE against a co-introduced TCV replicon, and that it likely accomplished this by
76 sequestering freshly translated p28 molecules into self-perpetuating p28 polymers. These earlier
77 observations raised at least three questions: (i) does the SIE activity of p28 require any specific domains
78 or amino acid residues in p28? (ii) can this replication-repressing SIE activity of p28 be decoupled from
79 its essential role in replication? (iii) can either of the p28 functions (replication and SIE) be decoupled
80 from the RdRP activity of p88? This last question is of interest as p88 encompasses the entire p28 at its
81 N-terminal 2/5 (Fig. 1A). The current study addresses these questions by identifying a 12 amino acid (aa)
82 region in p28 that is required for efficient SIE. Moreover, single aa changes within this region not only
83 enabled the decoupling of SIE activity of p28 from its replication function, but also the separation of the
84 replication function of p28 from that of p88. Our findings unveil novel mechanistic details of SIE
85 elicitation by TCV p28, and provide powerful new tools for further elucidation of the molecular basis of
86 TCV SIE.
87
88 **RESULTS**

89 **Deletion mutagenesis of p28-GFP fusion protein identifies a small region needed for robust SIE**
90 **elicitation**. We recently reported that a C-terminal GFP fusion bolsters the ability of p28 to elicit SIE to
91 TCV (15). Specifically, expression of the p28-GFP fusion protein in *Nicotiana benthamiana* cells abolished
92 the replication of TCV_sg2R, an mCherry-expressing TCV replicon, in the same cells, erasing the
93 replication-dependent mCherry fluorescence (15). Additionally, the strong replicational repression by
94 p28-GFP correlated with the occurrence of large, irregular green fluorescent foci in these cells (15).
95 These easy-to-monitor fluorescent phenotypes prompted us to use p28-GFP as the launch pad to map
96 domains in p28 essential for SIE elicitation. To systemically screen for these domains, we generated a
97 series of in-frame deletions within the p28 portion of p28-GFP (Fig. 2A). The effect of these deletions on
98 the SIE-eliciting ability of p28 was evaluated by expressing the mutant proteins in *N. benthamiana* cells,
99 and assessing the replication of the co-introduced TCV_sg2R replicon with Northern blot hybridizations.
100 In addition, we also monitored the replication-dependent diffuse mCherry fluorescence, as well as the
101 GFP-fluorescent mutant fusion proteins, using confocal microscopy.
102 As shown in Fig. 2B, deletion of the N-terminal half of the 250-aa p28 caused only minimal loss in
103 the SIE elicitation by p28-GFP, leading to a very modest recovery of TCV_sg2R replication (mutant Δ2-
104 125. Fig. 2A; and Fig. 2B, lanes 7 and 8). A specific N-terminal domain could not be delineated because
105 none of the smaller deletions within this region, including Δ2-36, Δ37-50, Δ37-100, Δ51-100, and Δ76-
106 125, led to detectable replication of TCV_sg2R (Fig. 2B, lanes 11-18; Fig. 2C, lanes 11-12). These results
107 suggest that, in the presence of the C-terminal GFP tag, the N-terminal half of p28 plays a modest role in
108 SIE elicitation. Consistent with this conclusion, the slightly shorter Δ2-100 mutation caused an SIE
109 release that is much weaker than Δ2-125, hence only occasionally detected (Fig. 2B, lanes 9 and 10; Fig.
110 2D, lanes 7 and 8).
111 Interestingly, the Δ2-155 mutant, which extends the Δ2-125 deletion for just 30 aa, permitted a
112 substantially higher level of TCV_sg2R replication (Fig. 2C, compare lanes 7-8 with 9-10). However, a

113 separate deletion of the 30 aa alone (Δ126-155) had a much weaker, though consistently detected
114 release of TCV_sg2R replication (Fig. 2C, compare lanes 13, 14 with lanes 7, 8). This suggested that loss
115 of SIE activity by the mutant Δ2-155 could be attributed to the additive or synergistic effect of two
116 regions – aa 2-125 and 126-155. Nevertheless, specific SIE-eliciting sequence motifs or aa residues
117 within the first 155 aa region could not be reliably identified with the GFP-tagged constructs.

118 Surprisingly, another relatively small deletion (Δ156-190, 35 aa in total) caused a loss of SIE activity
119 that rivaled the large Δ2-155 deletion (Fig. 2C, compare lanes 15, 16 with 7 and 8), thus identifying a
120 region with a relatively strong effect. Beyond aa 190, the entire C-terminal 60-aa region could be
121 removed without detectably compromising the SIE-eliciting activity of p28-GFP (Fig. 2D, Δ191-250, lanes
122 9 and 10). Indeed, a double deletion mutant combining the Δ2-100 and Δ191-250 deletions was no
123 worse than Δ2-100 alone at repressing TCV_sg2R replication (Fig. 2D, compare lanes 13, 14 with lanes 7
124 and 8). This further confirmed that the last 60-aa region was dispensable for SIE elicitation by p28-GFP.

125 Notably, the loss of SIE activity by many of the deletion mutants was accompanied by dramatic
126 changes in the intracellular behavior of mutant proteins. For example, although the SIE loss caused by
127 the Δ2-100 deletion was minimal, the Δ2-100-GFP formed large foci in substantially fewer cells than the
128 wild-type p28-GFP (Fig. 2E, panels 3 and 4), and instead exhibited a distribution resembling soluble GFP
129 in many cells (Fig. 2E, panel 4). Nevertheless, the smaller, more numerous foci formed by the GFP-
130 tagged Δ2-125, Δ126-155, and Δ156-190 proteins appear to be consistent with a requirement for larger
131 aggregates in SIE elicitation (Fig. 2E, panels 5, 7, and 8). Further supporting this idea is the observation
132 that the Δ2-155-GFP mutant protein was predominantly diffusely distributed, suggestive of a soluble
133 protein (Fig. 2E, panel 6).

134 **Additional deletions within the aa 156-190 region identify a 12-aa stretch with a significant role**
135 **in eliciting SIE.** That a substantial loss of SIE-eliciting activity could be inflicted by a mere 35-aa deletion
136 (Δ156-190) prompted us to further interrogate this small region using the p28-GFP fusion construct. To

137 this end, three smaller deletions (Δ156-170, Δ171-182, Δ183-190, deleting 15, 12, and 8 aa, respectively)
138 were generated and the resulting deletion mutants were analyzed for their ability to elicit SIE against
139 TCV_sg2R. As shown in Fig. 3A, neither Δ156-170 (lanes 9 and 10) nor Δ183-190 (lanes 13 and 14)
140 caused detectable loss of the SIE-eliciting activities. By contrast, deletion of aa 171-182 appeared to
141 account for most of the SIE loss observed with the Δ156-190 mutant.

142 We next investigated whether this 12-aa region contained any specific aa residue(s) critical for SIE
143 elicitation by generating three consecutive 4-aa deletions. As shown in Fig. 3B, lanes 9-14, all three
144 deletion mutants compromised the SIE-eliciting activity of p28-GFP to similar extents as the 12-aa
145 deletion mutant Δ171-182 (lanes 7 and 8). Therefore, it appears that the entire 12-aa region is needed
146 for eliciting a robust SIE. We then chose the last four aa residues of this region for single aa mutagenesis
147 and changed each of them to alanine (Fig. 3B, lanes 15-22). When these single aa mutants were
148 introduced into plant cells along with the TCV_sg2R replicon, only the F182A mutant caused a barely
149 detectable accumulation of TCV_sg2R RNAs (Fig. 3B, lanes 21 and 22), suggesting that the phenylalanine
150 to alanine change very weakly compromised the SIE-eliciting ability of p28-GFP.

151 Confocal microscopy showed that Δ156-170, Δ171-182, and Δ183-190 all abolished the ability to
152 form large aggregates (Fig. 3C, panels 3 and 4, also see Fig. 2E), and instead formed smaller, but more
153 numerous foci that sometimes arranged along cell boundaries. The Δ156-170 mutant was noteworthy
154 because it did allow occasional escape of red fluorescent cells, thus TCV_sg2R replication, even though
155 such low-level replication was not detected with Northern blotting (see above). This suggested that it
156 was important to use both Northern blotting and confocal microscopy to capture the full spectrum of
157 SIE-eliciting activities by these mutants.

158 Interestingly, the smaller, 4-aa deletion mutant Δ179-182 and the larger, 12-aa deletion mutant
159 Δ171-182 behaved highly similarly when inspected with confocal microscopy. Both permitted TCV_sg2R
160 replication in easily detectable numbers of cells, even though their replication levels as measured with

161 Northern blotting was much lower than controls without any p28-GFP derivatives (Fig. 2B, lanes 7-14).
162 Finally, three of the four single aa mutants, P179A, R180A, and V181A, formed large aggregates very
163 similar to those of wild-type p28-GFP, though smaller foci were also seen (Fig. 3C, panels 7-9). By
164 contrast, in cells treated with the F182A mutant, large aggregates were absent (Fig. 3C, panel 10).
165 Among these cells, replication-dependent red fluorescence was occasionally observed, thus confirming
166 the weak TCV_sg2R replication detected with Northern blotting (Fig. 2B, lanes 21-22).

167 **Replacing the C-terminal GFP with a double HA tag unveils additional regions important for SIE-**
168 **elicitation by p28**. Experiments using the p28-GFP fusion protein mutants identified the 12-aa region
169 spanning aa 171-182 as critically important for p28 to elicit SIE. But they failed to identify any other p28
170 regions that were specifically needed for SIE elicitation. These results contrasted with our previous
171 observations implicating the N-terminus of p28 in SIE elicitation. We showed earlier that fusing a short
172 G11 tag (25 aa) at the N-terminus rendered p28 incapable of eliciting SIE (15). We also found that a
173 truncated form of p28 missing the first 36 aa was no longer able to elicit SIE (15, 22). Did the C-terminal
174 GFP fusion in p28-GFP allow p28 to circumvent certain other critical regions, possibly through the
175 tendency of GFP to self-dimerize (23)? To address this question, we decided to adopt p28-HA, another
176 strong SIE-eliciting p28 variant with a C-terminal, duplicated hemagglutinin tag (15, 22). To this end, the
177 GFP in all deletion mutants described earlier was replaced with the HA tag and the resulting HA-tagged
178 mutants were retested for SIE induction.

179 As shown in Fig. 4A, the HA substitution indeed revealed a role for the N-terminal region in SIE
180 elicitation. The SIE-eliciting activity of p28-HA was not detectably weakened by deleting aa 51-100 or
181 191-250, suggesting that up to 110 amino acid residues of p28 could be removed without detectably
182 weakening SIE elicitation. However, this activity is clearly compromised by deletions of aa 2-36, 126-155,
183 and 156-190, and aa 37-100, 76-125, and 183-190 to lesser extents. Therefore, use of p28-HA as the

184 backbone permitted the identification of two additional p28 regions with potentially specific roles in SIE
185 elicitation, namely aa 2-50, and 126-155.

186 **Use of p28-HA reveals key amino acid residues within the aa 171-182 region critical for SIE**
187 **elicitation**. We next attempted to fine-map the 171-182 region, whose deletion compromised SIE in
188 both GFP and HA-tagged p28 variants, using HA-tagged mutants. As shown in Fig. 4B, use of the p28-HA
189 backbone revealed partial SIE losses caused by the Δ156-170 and Δ183-190 deletions (lanes 7, 8, 11, 12)
190 that were undetectable with the p28-GFP backbone (Fig. 3A, lanes 9, 10, and 13, 14). However, it is
191 important to note that only the deletion of the aa 171-182 core sequence fully recapitulated the
192 phenotype of the larger 156-190 deletion (Fig. 4B, compare lanes 5, 6 with 9, 10). Furthermore, each of
193 the three smaller, 4-aa deletions (Δ171-174, Δ175-178, and Δ179-182) within the aa 171-182 region
194 inflicted an SIE loss that is nearly identical to the 12-aa Δ171-182 (Fig. 4B, lanes 13-18).

195 We next re-examined the effect of four single aa substitutions using the p28-HA backbone. As
196 shown in Fig. 4C, the very weak SIE loss caused by the F182A mutation in p28-GFP background now
197 became easily detectable (lanes 15 and 16). Indeed, only the R180A mutation failed to inflict a
198 meaningful loss in the SIE-eliciting activity of p28-HA (lanes 11 and 12). By contrast, both P179A and
199 V181A mutations correlated with weak losses in SIE elicitation, with P179A being slightly less disruptive
200 than V181A (lanes 9, 10, 13 and 14).

201 **TCV replicons containing the V181A mutation overcome SIE in a substantial fraction of cells**. We
202 next wondered whether the single-aa mutations that compromised SIE in transiently expressed p28-GFP
203 and p28-HA had similar effects in TCV replicons. To resolve this question, we introduced the V181A and
204 F182A mutations into TCV_sG6H and TCV_sg2R, two TCV replicons that encode GFP [sG6H denotes GFP
205 with an N-terminal 6XHis tag (24)] and mCherry in place of CP, respectively (Fig. 1). These replicons were
206 then tested in co-infected cells to determine whether the mutations compromised SIE of TCV.

207 Although the GFP-encoding replicon (TCV_sG6H) appeared to replicate less robustly, and
208 produced much less sgRNAs (Fig. 5A, lane 2), it produced GFP at easily detectable levels (Fig. 2B, top
209 left), probably due to translational initiation from an internal ribosomal entry site identified recently
210 (25). Replicons with the V181A mutation (V181A_sG6H and V181A_sg2R) replicated to levels
211 comparable to wild-type replicons encoding wild-type p28 (and p88) (Fig. 5A, compare lanes 4, 5 with 2,
212 3, respectively). By contrast, the F182A mutation abrogated TCV replication to levels below the
213 detection limit of Northern blotting (lanes 6 and 7). Next, the V181A replicons were subjected to co-
214 infection experiments to assess the levels of SIE. As shown in Fig. 5B, while wild-type replicons exhibited
215 strong SIE that precluded the co-expression of GFP and mCherry in the same cells (top row), the V181A
216 replicons permitted such co-expression in approximately 19% of green- or red-fluorescent cells. These
217 results demonstrated that the same V181A mutation that compromised the ability of p28-HA to repress
218 TCV replication also compromised the ability of p28 to elicit SIE in TCV replicons.
219 **The F182A mutation disrupts the replication function of p28 but not p88**. Although in the p28-HA
220 background the F182A mutation more severely compromised SIE than V181A (Fig. 4), it also abolished
221 TCV replication when incorporated in replicons (Fig. 5). Since the p28 coding sequence is shared by p88
222 in the replicon context, it is possible that F182A disrupted the replication function of p28, or p88, or
223 both. To resolve this issue, we attempted to complement the replication of the F182A_sg2R replicon
224 using transiently expressed, tag-free p28 and p88 (Fig. 1B). As shown in Fig. 6A, F182A_sg2R replication
225 was restored to easily detectable levels by transiently expressed p28 (compare lanes 9, 10 to 5, 6), but
226 not p88 (lanes 13 and 14). Therefore, the F182A mutation primarily disrupted the auxiliary replication
227 function of p28. While perturbation of p88 function by F182A could not be completely ruled out, such
228 perturbation did not abolish TCV replication. Taken together, the F182A mutation severely debilitated
229 the replication function of p28, but not p88. In conclusion, this mutation decouples the replication
230 functions of p28 and p88.

231 **An F182A-containing replicon, upon replicational complementation, exerts robust SIE against a**
232 **wild-type replicon.** We next examined whether the replicational defect of the F182A-containing
233 replicons could be complemented by another replicon encoding a replication-competent p28, and
234 whether the p28(F182A) protein produced by the complemented replicon might exert SIE against the
235 replicon that provided the complementing p28. To answer this question, we paired the F182A_sg2R
236 replicon with TCV_sG6H or V181A_sG6H, in co-infections of *N. benthamiana* cells. As shown in Fig. 6B,
237 panels 4 and 6, both TCV_sG6H and V181A_sG6H replicons complemented the F182A defect, enabling
238 an approximately ten-fold increase in the number of cells replicating F182A_sg2R (Fig. 6B, panels 3, 4,
239 and 6; Fig. 6C, red bars in groups 3, 4, and 6).
240 However, complementation by the two GFP-encoding replicons led to starkly different SIE
241 phenotypes. The complementation by TCV_sG6H, which encodes a wild-type p28, gave rise to mCherry-
242 expressing cells that never contained GFP fluorescence (Fig. 6B, panel 4; Fig. 6C, group 4). Conversely,
243 the GFP-expressing cells also never contained mCherry. Because the TCV_sG6H construct must reside in
244 the same cells as the F182A_sg2R construct in order to supply the replication-complementing wild-type
245 p28, these observations strongly suggested that the p28(F182A) protein, now produced by the
246 replicating F182A_sg2R replicon, exerted a powerful SIE to block TCV_sG6H replication. Note that we
247 have shown in a previous study (15) that commencement of TCV replication in different agro-infiltrated
248 *N. benthamiana* cells was highly asynchronous, meaning many cells could translate wild-type p28
249 protein from the 2X35S-driven replicon transcripts, but failed to immediately embark on replicon
250 replication. These cells would provide the p28 protein to complement the replication of F182A_sg2R,
251 the latter then turn around to exert SIE against the p28-providing wild-type replicon.
252 The assertion that both F182A_sg2R and TCV_sG6H constructs must have been present in those
253 red fluorescent cells is further bolstered by the contrasting SIE phenotype observed from the
254 complementation mediated by V181A_sG6H (Fig. 6B, panel 6; Fig. 6C), as these experiments were

255 carried out in parallel. Specifically, when the replication of F182A_sg2R was complemented with the
256 V181A_sG6H replicon, approximately one half of the red fluorescent cells also contained GFP
257 fluorescence. This probably reflected the partial loss of SIE-eliciting capacity by the p28(V181A) protein
258 (Fig. 5B. Also see Fig. 6B, panel 5). But this result also demonstrated that two different replicon
259 constructs readily enter the same agro-infiltrated cells. Together these results indicated that when
260 expressed from a replicating replicon, the p28(F182A) protein is fully capable of exerting a strong SIE
261 against another replicon in the same cells, despite its inability to facilitate replication on its own.
262 Therefore, in addition to decoupling the replication function of p28 and p88, the F182A mutation also
263 decoupled the SIE function and replication function of p28 – but in a manner diametrical to the V181A
264 mutation.
265
266 **DISCUSSION**
267 SIE protects host cells from being sequentially infected by the same virus. Although use of SIE in
268 controlling plant virus diseases has been extensively documented, its underlying molecular mechanism,
269 and its evolutionary rationale, remain poorly understood (13). Using the model virus TCV, we have
270 previously established that SIE occurred inside the super-invaded cells, and acted to repress the
271 replication of the superinfecting viral genomes (15, 26). We further discovered that SIE in TCV infections
272 is mediated by a single, TCV-encoded protein (p28) that is also needed for TCV replication, likely through
273 the formation of a self-perpetuating polymeric state that sequesters homologous p28 monomers. This
274 model raised the possibility that SIE exists to ensure that progeny genomes of a virus are excluded from
275 additional rounds of replication, thus minimizes error accumulation within single cells (17). By extension,
276 cells invaded by many copies of the same virus simultaneously, frequently in the form of collective
277 infectious units (27–30), likely also experience similar molecular events that ensure only a small number
278 of the entered genomes is allowed to replicate, and be exposed to cellular level selections. If this is true,

279 then viral mutants that weaken SIE are expected to relax this restriction, allowing more viral genomes to
280 replicate for multiple cycles in the same cells, causing faster error accumulation in viral populations, and
281 likely more swift collapse of these populations.

282 The current study was designed to test the predictions of our working hypothesis by first
283 identifying mutations within TCV p28 that compromise SIE. Our systematic deletion mutagenesis of p28,
284 using two different C-terminally tagged forms of p28 as the backbones, allowed us to narrow down the
285 SIE-eliciting activity of p28 to three regions: aa 2-50, 126-155, and 156-190. The aa 156-190 region was
286 then further interrogated because deletion of this region caused a consistent loss of SIE in both p28-GFP
287 and p28-HA backgrounds. These efforts ultimately led to the identification of two amino acid residues,
288 namely valine (V) and phenylalanine (F) at positions 181 and 182, respectively, whose replacement by
289 alanine (A) in replicons led to the decoupling of p28 replication function and its SIE elicitation function.

290 The apparent inconsistency of the defects caused by the F182A mutation in different construct
291 contexts warrants further discussions. Specifically, in transiently expressed p28-GFP as well as p28-HA
292 contexts, F182A weakened SIE to levels detectable with Northern blotting. Yet replicons containing the
293 same mutation exhibited no loss in SIE elicitation, even though the p28(F182A) mutant protein was
294 unable to support replication on its own. This discrepancy raises the important question of whether the
295 SIE-eliciting capacity of transiently expressed p28 derivatives reliably predicts the same activity of
296 replicon-borne p28. To reconcile this discrepancy, we propose as a working hypothesis that the F182A
297 mutation accelerates the turnover of the p28 protein. Below we provide the rationale for this
298 hypothesis.

299 We observed previously that p28 without any fusion tags only modestly repressed the replication
300 of a TCV replicon when transiently expressed, but was strongly repressive when expressed from another
301 TCV replicon (15, 17). This was likely due to the difference in the amount of p28 protein translated in
302 these two situations. The abundance of p28 mRNA transcribed from transient expression constructs was

303 far lower than from the gRNA of a replicating TCV replicon, suggesting that the concentration of p28
304 protein would also be substantially lower, thus diminishing the formation of the SIE-eliciting polymeric
305 state. Accordingly, the C-terminally tagged p28-GFP and p28-HA could have elicited robust SIE by
306 increasing the p28 concentration indirectly, by slowing down the turnover of the fusion proteins.
307 Conversely, the SIE-eliciting activity of these fusion proteins would be weakened by the F182A mutation,
308 if such a mutation accelerates p28 turnover. Importantly, the SIE defect of this mutation would be
309 neutralized if the increased translation from replicons more than offset the faster turnover, thus
310 explaining the maintenance of strong SIE in F182A replicons. Furthermore, this hypothesis would
311 probably also explain the replication defect of p28(F182A) if, as we proposed earlier, the replication
312 function of p28 also entails lateral polymerization that could only be sustained when a concentration
313 threshold is reached (17). We plan to test this hypothesis in the near future, once a high quality p28
314 antibody becomes available.
315 To summarize, the current study identifies two single aa mutations in TCV p28 that differentially
316 impaired the two opposite functions of p28 – replication and SIE elicitation, hence decoupling these two
317 functions of p28. These mutations will allow us to investigate the impact of SIE in the rate of mutation
318 accumulation in TCV populations, providing insights regarding the evolutionary rationale for preserving
319 SIE functionality in virus infections. These investigations would in turn unravel potential targets for
320 antiviral therapy, and prompt novel management strategies for virus diseases.
321
322 **MATERIALS AND METHODS**
323 **Constructs**. Constructs 2X35S::TCV_sg2R, p28-HA, p28 (tag-free), and Core35S::p88 (tag-free)
324 were described in previous studies (15, 22). The 2X35S::p28-GFP construct was a slightly modified
325 version of the previous p28-GFP. The new version replaced the NotI site (GCGGCCGCA) linking p28 and
326 GFP coding sequences with a BamHI site plus three additional nts (GGATCCGGA). Nearly all deletion

327 mutants, as well as single aa substitution mutants, were generated using synthetic gBlocks fragments
328 (IDT, Coralville, IA) that were integrated into various backbone plasmids (e.g. p28-GFP, p28-HA, or
329 TCV_sg2R) using Gibson Assembly cloning (NEB, Ipswich, MA). The identities of all new constructs were
330 verified with Sanger sequencing.

331 **Agro-infiltration**. Upon verification, all of the constructs were introduced into *Agrobacterium*
332 *tumefaciens* strain C58C1 with electroporation (31, 32). To carry out the experiments described in the
333 Results section, various combinations of *Agrobacterium* suspensions were mixed together and delivered
334 into *N. benthamiana* leaves as described (22, 26, 31, 33). A p19-expressing *Agrobacterium* strain was
335 included in all combinations to alleviate RNA silencing-mediated mRNA degradation.

336 **RNA extraction and Northern blotting**. Total RNA was extracted from agro-infiltrated *N.*
337 *benthamiana* leaves using the Direct-zol RNA Miniprep kit (Zymo Research, Irvine, CA). To ensure
338 consistency, four equivalent leaf sections derived from infiltrated leaves of four different plants were
339 pooled before RNA extraction. The RNA extraction procedure included a DNase treatment step that
340 removes DNA contamination. The RNA was then quantified with NanoDrop and subjected to Northern
341 blotting as described (22, 26, 31, 33).

342 **Confocal microscopy and quantification of fluorescent cells.** Confocal microscopic observations
343 were carried out using a Leica Confocal microscope (TCS SP5) available at Molecular and Cellular Imaging
344 Center at the Ohio Agricultural Research and Development Center, The Ohio State University. To
345 quantify the percentage of cells expressing GFP, mCherry, or both (Fig. 5), the agro-infiltrated *N.*
346 *benthamiana* leaf sections were photographed under the confocal microscope, at the low magnification
347 (10X), and for three separate channels (GFP, mCherry, and merged). For each treatment, five
348 independent leaf sections were photographed, resulting in 15 images. These images, typically
349 encompassing 40-50 cells, were then divided into 100 equal subdivisions with the grid line feature of the
350 PhotoShop software. Subdivisions that are more than 50% filled with a given fluorescence (GFP,

351 mCherry, or both) were counted as positive for the respective protein, the total counts of which
352 represent a percentage in a given image. For each treatment five counts were obtained, and standard
353 deviation were computed using these counts.
354
355 **FIGURE LEGENDS**
356 **Figure 1.** TCV genome organization, and the configurations of the constructs used in this study. **A:**
357 the organization of the 4,054 nt single-stranded, positive sense (+) TCV genome. The various boxes with
358 labels within (e.g. p28, p88, p8, p9, p38) denote the proteins encoded by the TCV genome, with the
359 boundaries of some ORFs shown. The three 3' proximal proteins (p8, p9, and p38) are translated from
360 two subgenomic RNAs (sgRNA1 and 2). **B**: representative constructs used in this study. Most constructs
361 were equipped with the strong 35S promoter with the enhancer duplicated (2X35S) in order to ensure
362 efficient transcription. Only the last, p88-expressing construct was driven by the relatively weak core
363 35S promoter as high level of p88 translation was shown to repress TCV replication (22). The top most
364 construct is a replicon shown previously to launch TCV replication in plant cells, leading to mCherry
365 expression from the sgRNA2 (19, 33). All other constructs direct transient expression of the respective
366 proteins in the absence of TCV replication.
367 **Figure 2**. Deletion mutagenesis on the p28-GFP backbone identifies the aa 156-190 region as
368 needed for robust SIE. **A**: diagrams of deletion mutants of p28-GFP showing their respective deleted
369 regions. **B, C, D:** Northern blotting results showing the levels of replicational repression imposed on the
370 TCV_sg2R replicon by p28-GFP and its deletion mutants. The p19 silencing suppressor was included to
371 mitigate the impact of RNA silencing. The double loadings represented two independent samples
372 extracted from different leaves. The positions of gRNA, sgRNA1 and 2 were highlighted with arrows (g,
373 sg1, sg2). EB: ethidium bromide-stained gel. **E:** confocal images of *N. benthamiana* leaf cells treated with
374 select p28-GFP deletion mutants along with the TCV_sg2R replicon.

375 **Figure 3**. Mapping the aa 156-190 region of p28-GFP with smaller deletions and single aa
376 exchanges identifies aa 171-182 as the key determinant of SIE. **A and B**: Northern blots showing the
377 levels of replicational repression imposed on the TCV_sg2R replicon by various smaller deletion and
378 single aa mutants of p28-GFP. **C:** confocal images of *N. benthamiana* leaf cells treated with select p28-
379 GFP mutants along with the TCV_sg2R replicon.

380 **Figure 4.** Use of the p28-HA backbone reveals additional regions contributing to SIE elicitation by
381 p28. All panels are Northern blots showing the levels of replicational repression imposed on the
382 TCV_sg2R replicon by various mutants of p28-HA.

383 **Figure 5**. Replication and SIE of mutant replicons with the V181A and F182A mutations. **A:**
384 Northern blot showing the replication (lanes 4-7) and SIE (lanes 10-13) of the mutant replicons encoding
385 different fluorescent proteins (GFP or mCherry). **B:** confocal images showing robust SIE between two
386 wild-type replicons (top panels), and the partially compromised SIE between the two V181A mutant
387 replicons. The quantification was based on five independent leaf areas each containing 40-50 cells. See
388 Materials and Methods for details. G = GFP-fluorescent cells, R = mCherry-fluorescent cells, G+R = cells
389 containing both GFP and mCherry.

390 **Figure 6**. In replicons, the F182A mutation selectively abrogates the replication function of p28,
391 but not its ability to elicit SIE. **A:** Northern blot showing that the replicational defect of the F182A
392 replicon was complemented by transiently expressed p28 but not p88. **B:** confocal images showing that
393 the replicational defect of the F182A replicon was also complemented by co-introduced wild-type and
394 V181A replicons, and the successfully complemented F182A replicon exerted robust SIE against the wild-
395 type replicon. **C:** quantification of replicational complementation and SIE of the F182A replicon. The
396 numbering of the experimental sets corresponded to Fig. 6B. In all sets leaf areas of 40-50 cells each
397 were chosen from five different leaves and counted for cells with different fluorescence (GFP, mCherry,
398 or both).

399

400 **ACKNOWLEDGMENTS**

401 We thank the labs of Drs. Lucy Stewart and Peg Redinbaugh for generous equipment sharing, and
402 other members of the Qu lab for stimulating discussions. This study was supported by a grant from the
403 National Science Foundation (#1758912), a SEEDS grant from the Ohio Agricultural Research and
404 Development Center, Graduate Assistantships from OSU and OARDC to Q.G. and R.S., respectively, as
405 well as tuition assistances to S.Z., R.S., and Q.G. from the Department of Plant Pathology, OSU.

406

407 **LITERATURE**

408 1. Nethe M, Berkhout B, van der Kuyl AC. 2005. Retroviral superinfection resistance. Retrovirology
409 2:52.

410 2. Schaller T, Appel N, Koutsoudakis G, Kallis S, Lohmann V, Pietschmann T, Bartenschlager R. 2007.
411 Analysis of Hepatitis C Virus Superinfection Exclusion by Using Novel Fluorochrome Gene-Tagged
412 Viral Genomes. J Virol 81:4591.

413 3. Tscherne DM, Evans MJ, von Hahn T, Jones CT, Stamataki Z, McKeating JA, Lindenbach BD, Rice
414 CM. 2007. Superinfection exclusion in cells infected with hepatitis C virus. J Virol 81:3693–3703.

415 4. Zou G, Zhang B, Lim P-Y, Yuan Z, Bernard KA, Shi P-Y. 2009. Exclusion of West Nile Virus
416 Superinfection through RNA Replication. J Virol 83:11765.

417 5. Simon KO, Cardamone JJ, Whitaker-Dowling PA, Youngner JS, Widnell CC. 1990. Cellular
418 mechanisms in the superinfection exclusion of vesicular stomatitis virus. Virology 177:375–379.

419 6. Julve JM, Gandía A, Fernández-del-Carmen A, Sarrion-Perdigones A, Castelijns B, Granell A, Orzaez
420 D. 2013. A coat-independent superinfection exclusion rapidly imposed in Nicotiana benthamiana

421 cells by tobacco mosaic virus is not prevented by depletion of the movement protein. Plant Mol
422 Biol 81:553–564.

423 7. Dietrich C, Maiss E. 2003. Fluorescent labelling reveals spatial separation of potyvirus populations
424 in mixed infected Nicotiana benthamiana plants. J Gen Virol 84:2871–2876.

425 8. Bergua M, Zwart MP, El-Mohtar C, Shilts T, Elena SF, Folimonova SY. 2014. A viral protein mediates
426 superinfection exclusion at the whole-organism level but is not required for exclusion at the
427 cellular level. J Virol 88:11327–11338.

428 9. Miyashita S, Kishino H. 2010. Estimation of the size of genetic bottlenecks in cell-to-cell movement
429 of soil-borne wheat mosaic virus and the possible role of the bottlenecks in speeding up selection
430 of variations in trans-acting genes or elements. J Virol 84:1828–1837.

431 10. Takahashi T, Sugawara T, Yamatsuta T, Isogai M, Natsuaki T, Yoshikawa N. 2007. Analysis of the
432 Spatial Distribution of Identical and Two Distinct Virus Populations Differently Labeled with Cyan
433 and Yellow Fluorescent Proteins in Coinfected Plants. Phytopathology 97:1200–1206.

434 11. Folimonova SY. 2012. Superinfection Exclusion Is an Active Virus-Controlled Function That Requires
435 a Specific Viral Protein. J Virol 86:5554.

436 12. Ziebell H, Carr JP. 2010. Cross-Protection, p. 211–264. *In* Advances in Virus Research. Elsevier.

437 13. Zhang X-F, Qu F. 2016. Cross Protection of Plant Viruses: Recent Developments and Mechanistic
438 Implications, p. 241–250. *In* Wang, A, Zhou, X (eds.), Current Research Topics in Plant Virology.
439 Springer International Publishing, Cham.

440 14. Folimonova SY. 2013. Developing an understanding of cross-protection by Citrus tristeza virus.
441 Front Microbiol 4:76.

442 15. Zhang X-F, Sun R, Guo Q, Zhang S, Meulia T, Halfmann R, Li D, Qu F. 2017. A self-perpetuating
443 repressive state of a viral replication protein blocks superinfection by the same virus. PLOS Pathog
444 13:e1006253.

445 16. Tatineni S, French R. 2016. The Coat Protein and NIa Protease of Two Potyviridae Family Members
446 Independently Confer Superinfection Exclusion. J Virol 90:10886–10905.

447 17. Zhang X-F, Zhang S, Guo Q, Sun R, Wei T, Qu F. 2018. A New Mechanistic Model for Viral Cross
448 Protection and Superinfection Exclusion. Front Plant Sci 9.

449 18. White KA, Skuzeski JM, Li W, Wei N, Morris TJ. 1995. Immunodetection, Expression Strategy and
450 Complementation of Turnip Crinkle Virus p28 and p88 Replication Components. Virology 211:525–
451 534.

452 19. Cao M, Ye X, Willie K, Lin J, Zhang X, Redinbaugh MG, Simon AE, Morris TJ, Qu F. 2010. The Capsid
453 Protein of Turnip Crinkle Virus Overcomes Two Separate Defense Barriers To Facilitate Systemic
454 Movement of the Virus in Arabidopsis. J Virol 84:7793–7802.

455 20. Zhang X, Zhang X, Singh J, Li D, Qu F. 2012. Temperature-Dependent Survival of Turnip Crinkle
456 Virus-Infected Arabidopsis Plants Relies on an RNA Silencing-Based Defense That Requires DCL2,
457 AGO2, and HEN1. J Virol 86:6847–6854.

458 21. Qu F, Ye X, Morris TJ. 2008. Arabidopsis DRB4, AGO1, AGO7, and RDR6 participate in a DCL4-
459 initiated antiviral RNA silencing pathway negatively regulated by DCL1. Proc Natl Acad Sci
460 105:14732–14737.

461 22. Zhang S, Sun R, Guo Q, Zhang X-F, Qu F. 2019. Repression of turnip crinkle virus replication by its
462 replication protein p88. Virology 526:165–172.

463 23. Shaner NC, Steinbach PA, Tsien RY. 2005. A guide to choosing fluorescent proteins. Nat Methods
464 2:905–909.

465 24. Powers JG, Sit TL, Qu F, Morris TJ, Kim K-H, Lommel SA. 2008. A Versatile Assay for the
466 Identification of RNA Silencing Suppressors Based on Complementation of Viral Movement. Mol
467 Plant Microbe Interact 21:879–890.

468 25. May J, Johnson P, Saleem H, Simon AE. 2017. A Sequence-Independent, Unstructured Internal
469 Ribosome Entry Site Is Responsible for Internal Expression of the Coat Protein of Turnip Crinkle
470 Virus. J Virol 91:e02421-16.

471 26. Zhang X-F, Guo J, Zhang X, Meulia T, Paul P, Madden LV, Li D, Qu F. 2015. Random Plant Viral
472 Variants Attain Temporal Advantages During Systemic Infections and in Turn Resist other Variants
473 of the Same Virus. Sci Rep 5.

474 27. Chen Y-H, Du W, Hagemeijer MC, Takvorian PM, Pau C, Cali A, Brantner CA, Stempinski ES,
475 Connelly PS, Ma H-C, Jiang P, Wimmer E, Altan-Bonnet G, Altan-Bonnet N. 2015.
476 Phosphatidylserine Vesicles Enable Efficient En Bloc Transmission of Enteroviruses. Cell 160:619–
477 630.

478 28. Mirabelli C, Wobus CE. 2018. All Aboard! Enteric Viruses Travel Together. Cell Host Microbe
479 24:183–185.

480 29. Andreu-Moreno I, Sanjuán R. 2018. Collective Infection of Cells by Viral Aggregates Promotes Early
481 Viral Proliferation and Reveals a Cellular-Level Allee Effect. Curr Biol 28:3212-3219.e4.

482 30. Miyashita S, Ishibashi K, Kishino H, Ishikawa M. 2015. Viruses Roll the Dice: The Stochastic Behavior
483 of Viral Genome Molecules Accelerates Viral Adaptation at the Cell and Tissue Levels. PLOS Biol
484 13:e1002094.

485 31. Qu F, Ren T, Morris TJ. 2003. The Coat Protein of Turnip Crinkle Virus Suppresses
486 Posttranscriptional Gene Silencing at an Early Initiation Step. J Virol 77:511–522.

487 32. Qu F, Ye X, Hou G, Sato S, Clemente TE, Morris TJ. 2005. RDR6 Has a Broad-Spectrum but
488 Temperature-Dependent Antiviral Defense Role in Nicotiana benthamiana. J Virol 79:15209–
489 15217.

490 33. Zhang X-F, Sun R, Guo Q, Zhang S, Meulia T, Halfmann R, Li D, Qu F. 2017. A self-perpetuating
491 repressive state of a viral replication protein blocks superinfection by the same virus. PLOS Pathog
492 13:e1006253.

493

494

495

496

Guo et al., 2019 Fig. 1

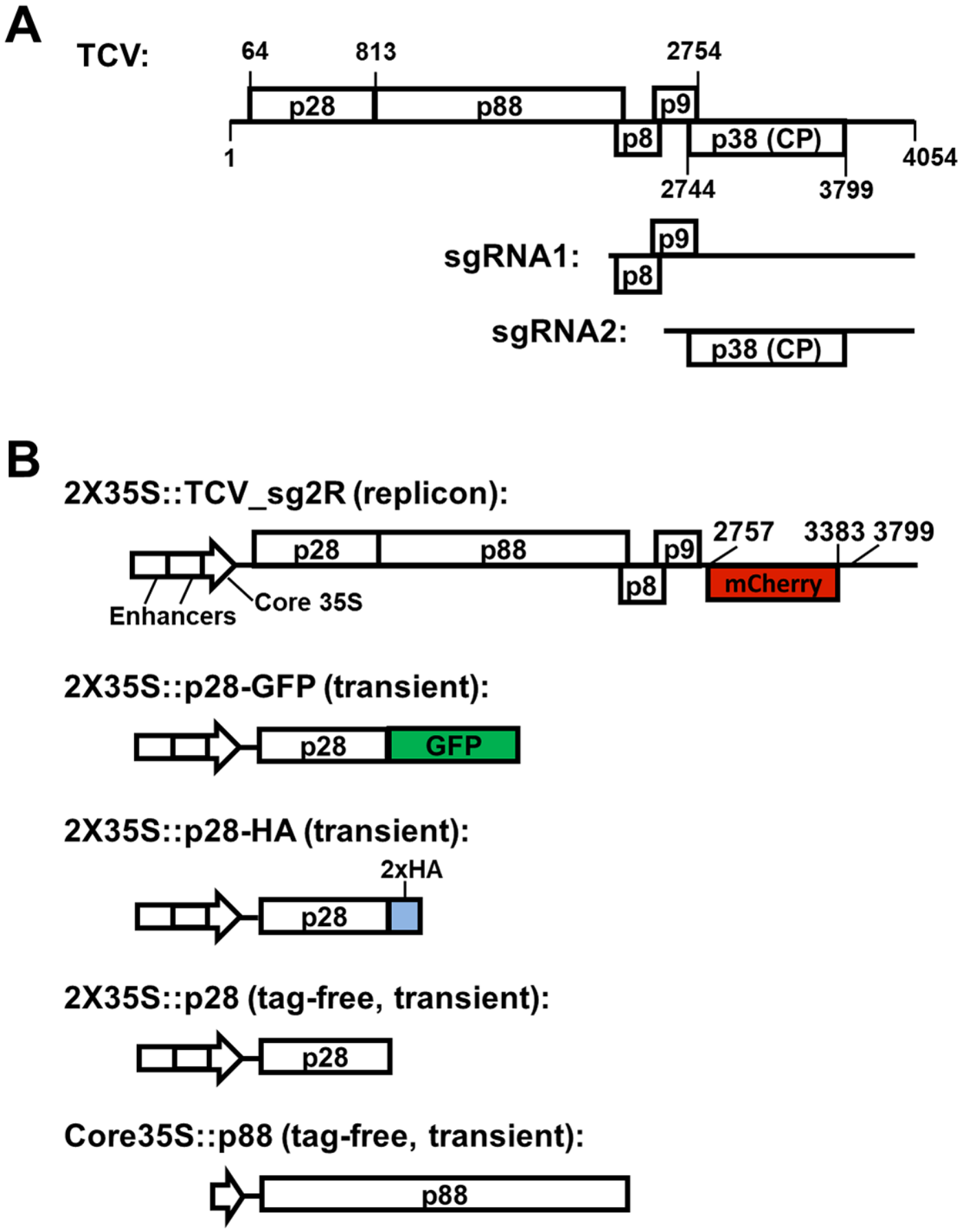

Guo et al., 2019 Fig. 2

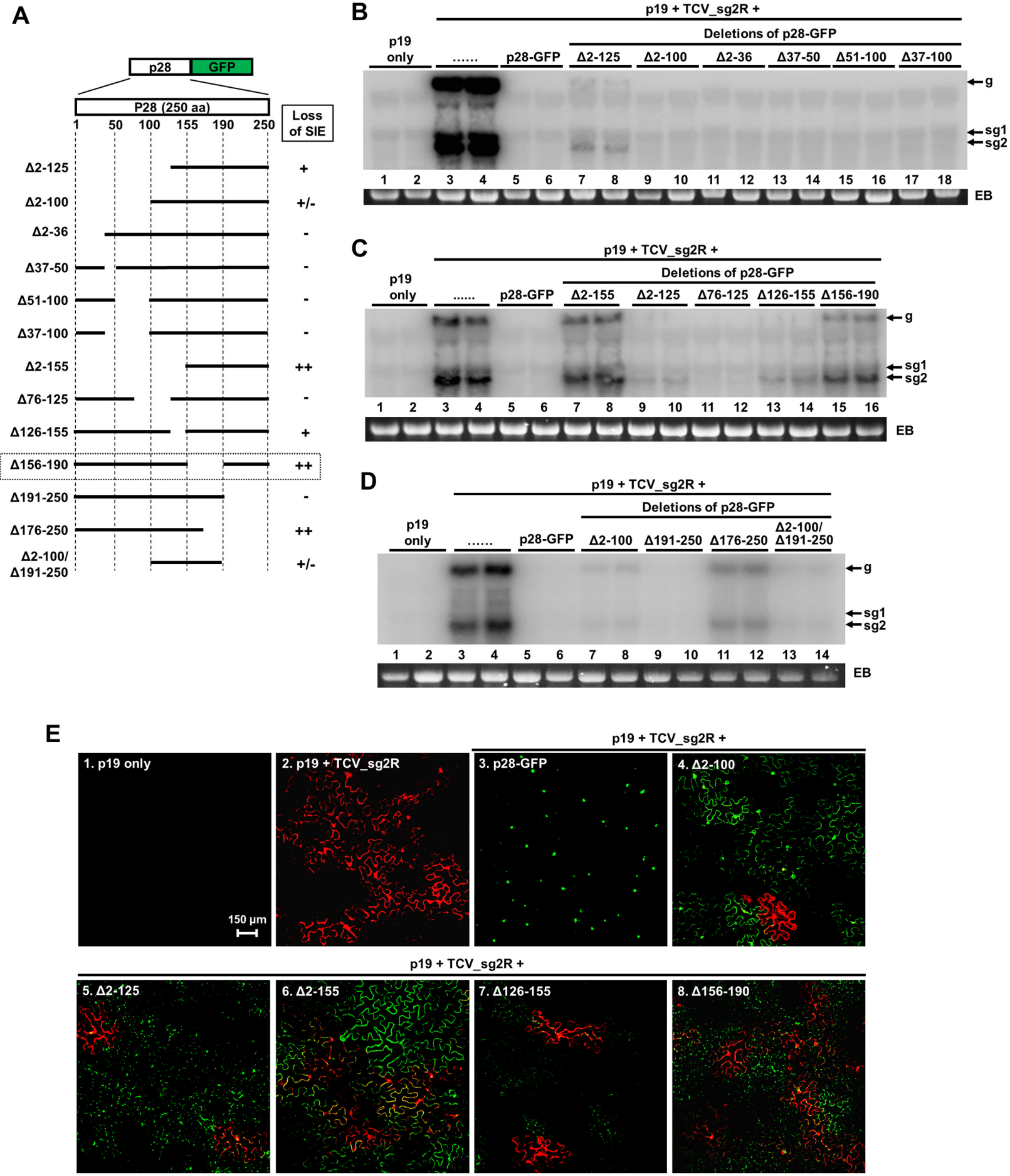

Guo et al., 2019 Fig. 3

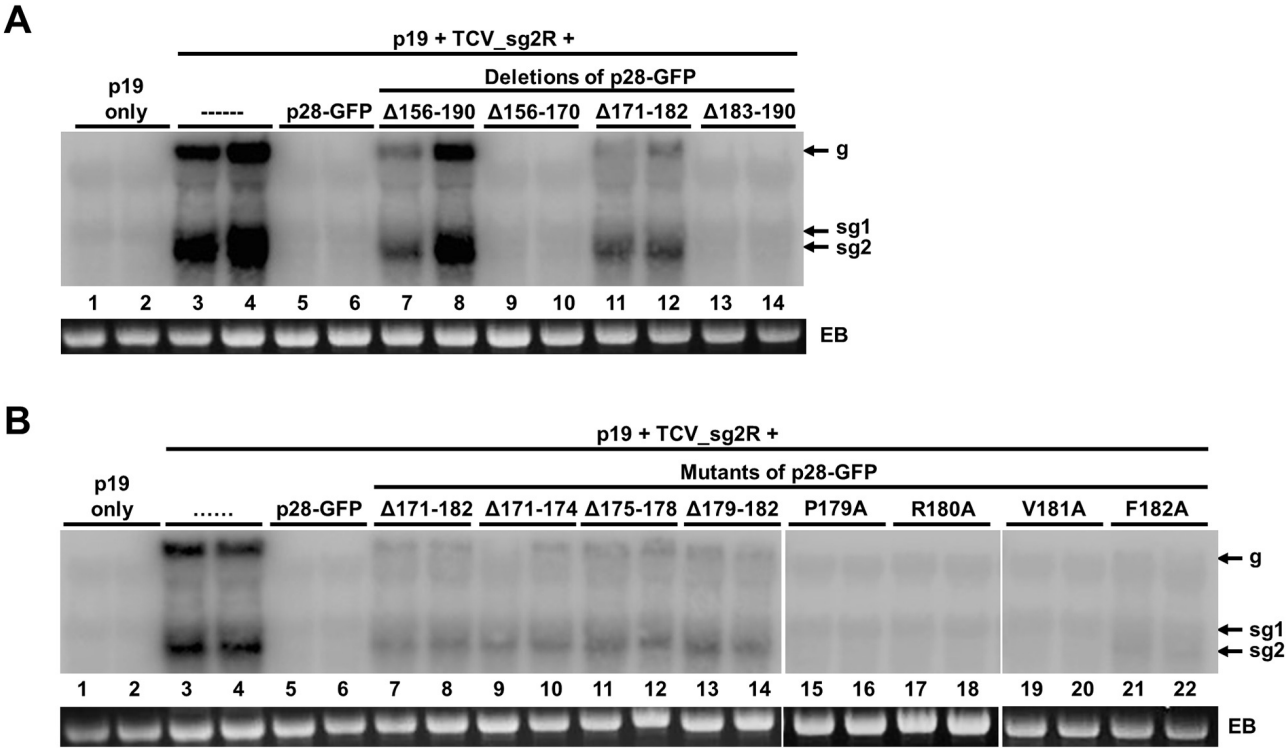


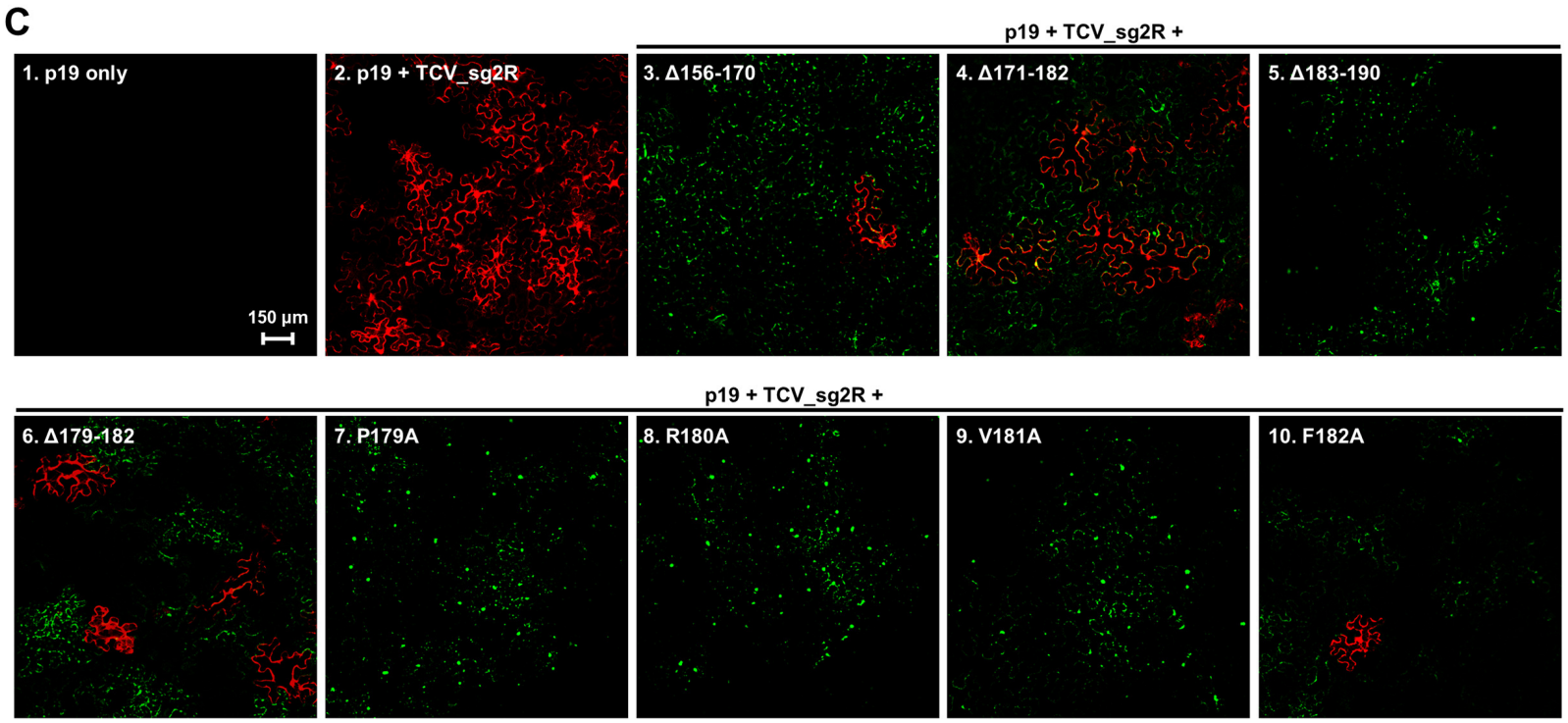

Guo et al., 2019 Fig. 4

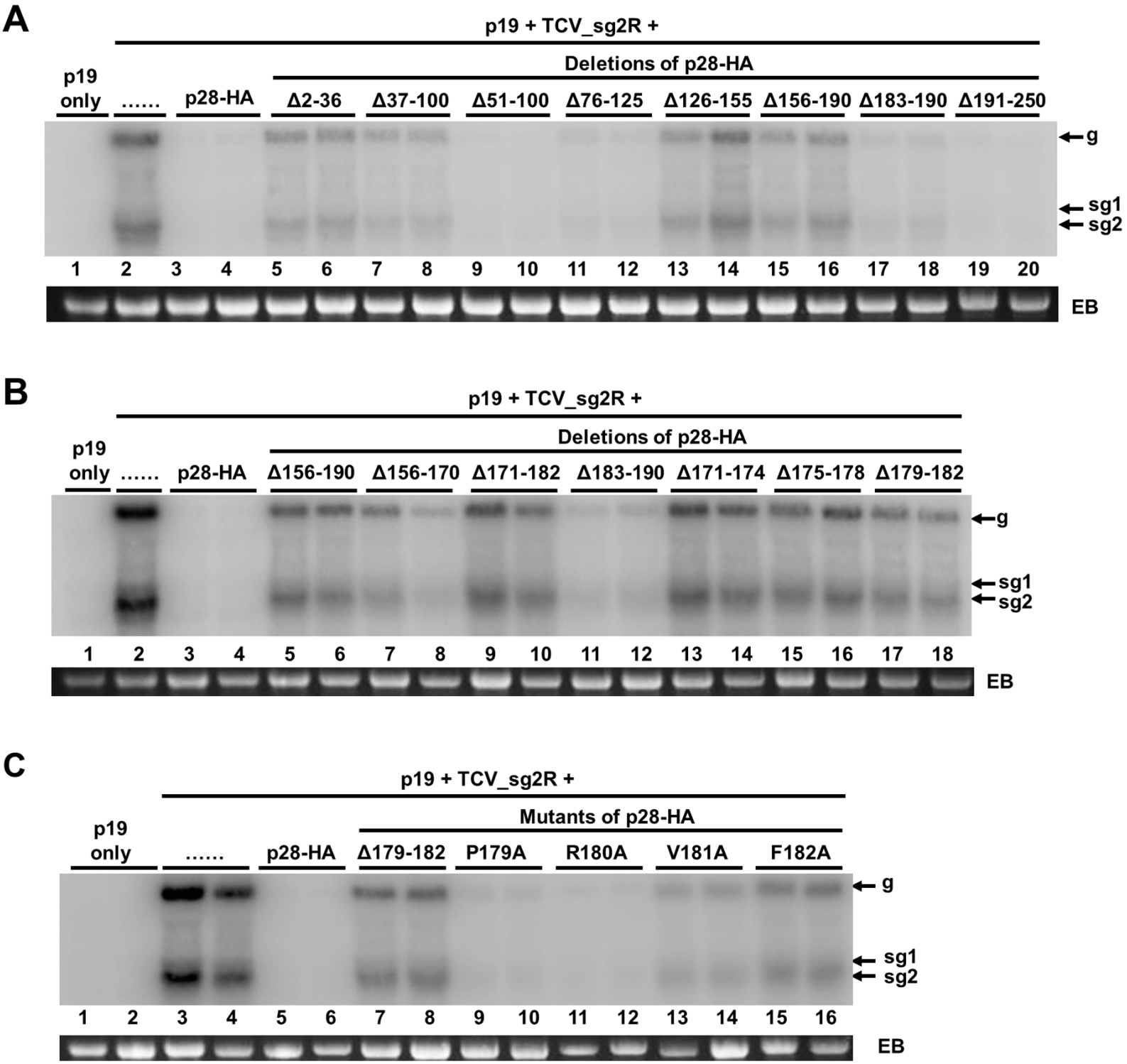

Guo et al., 2019 Fig. 5

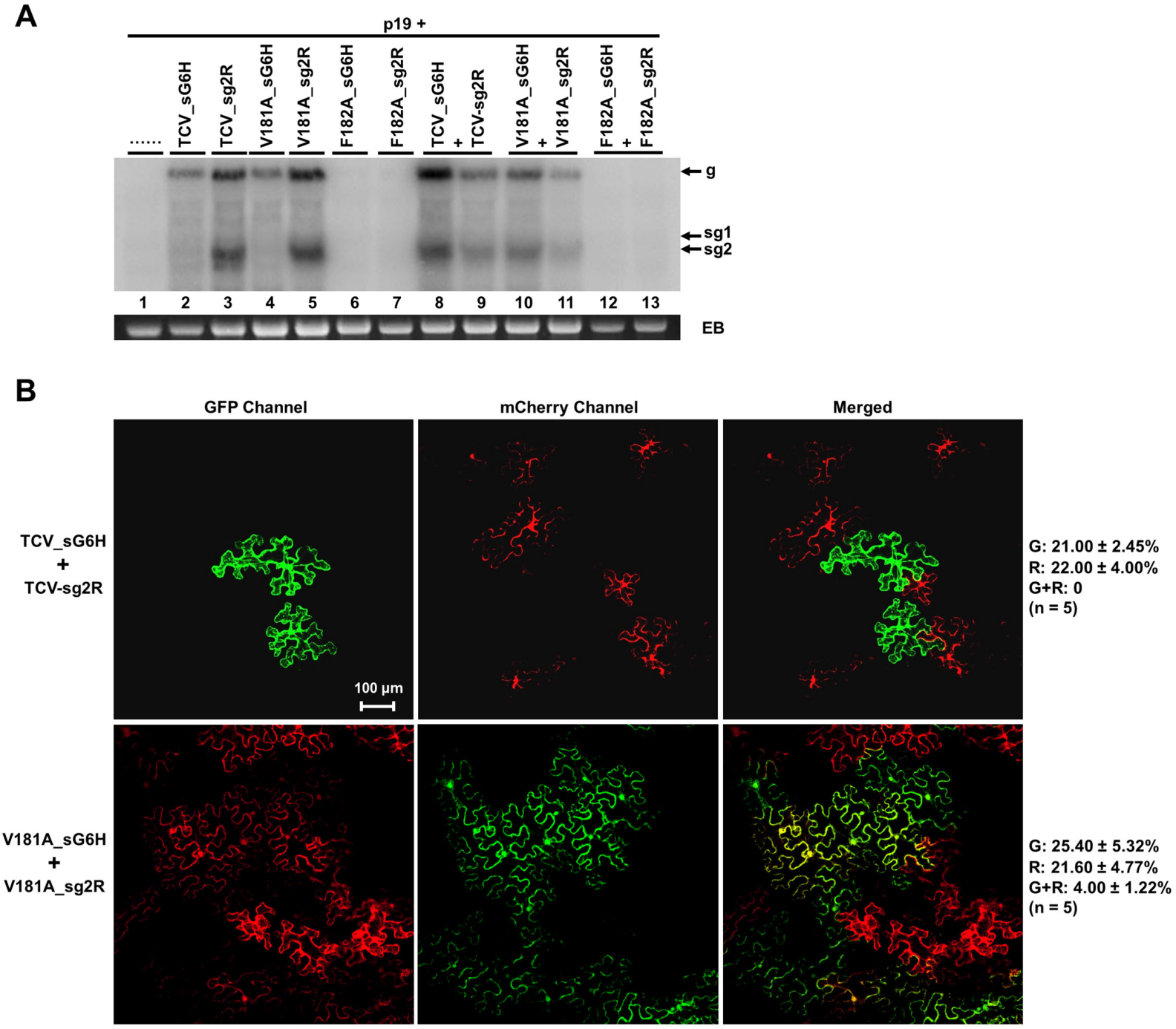
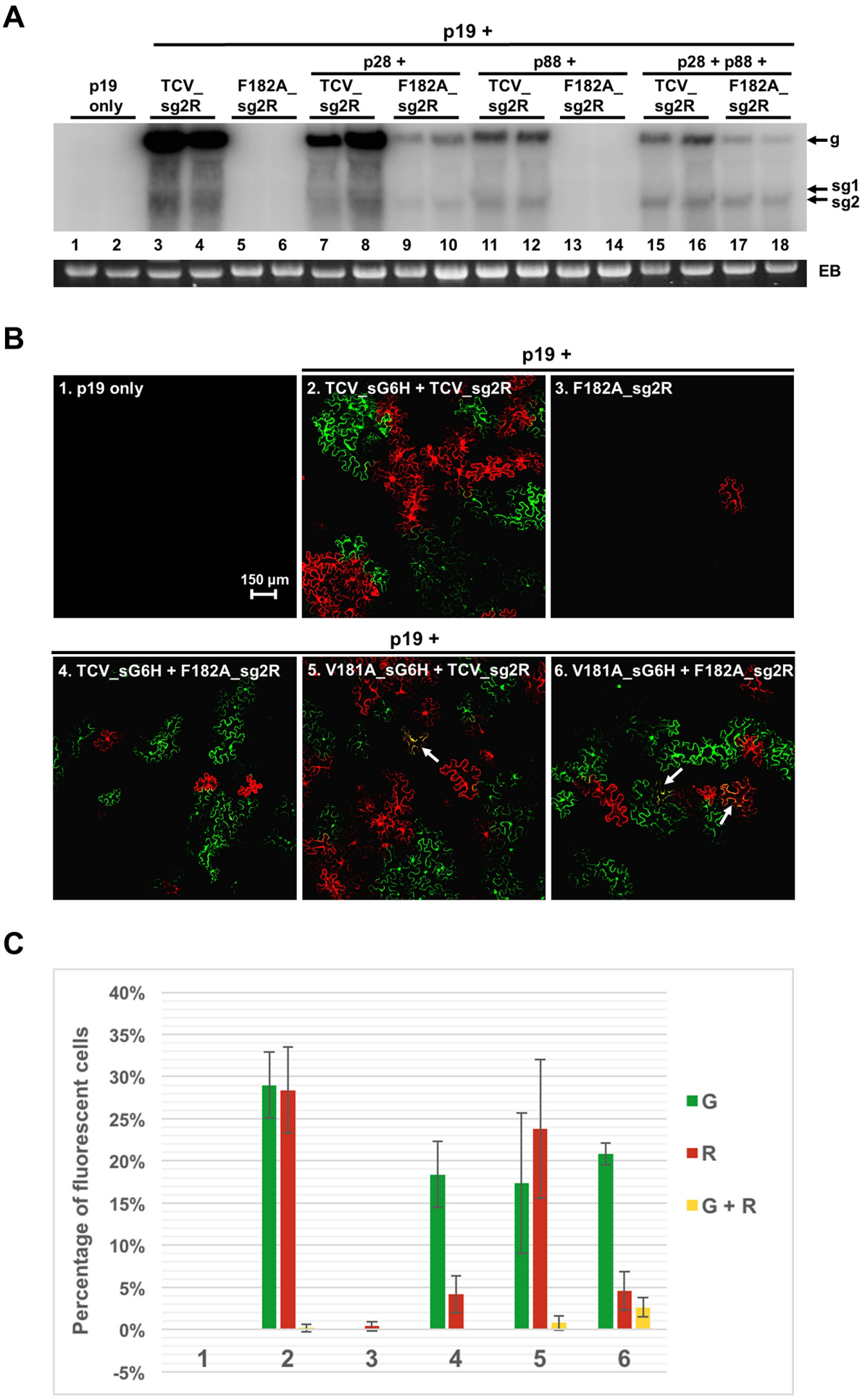
Guo et al., 2019 Fig. 6